Simulation of LiDAR, Unmanned Ground Vehicles, and Neural Networks for Leaf Area Estimation in Orchards

Harold Murcia, Simon Lacroix

Simulation of LiDAR, Unmanned Ground Vehicles, and Neural Networks for Leaf Area Estimation in Orchards

H. Murcia Moreno[1, 2] and S. Lacroix[1]

[1]LAAS-CNRS, Université de Toulouse, CNRS, Toulouse, France

[2]Facultad de Ingeniería, Universidad de Ibagué, Colombia

hfmurciamo@laas.fr

Abstract

The leaf area index (LAI) is vital for assessing plant photosynthetic activity, crucial for optimising orchard management. This study presents a method to estimate leaf area density (LAD) variations and tree LAI using LiDAR data from unmanned ground vehicles (UGVs). Combining 3D tree reconstruction with neural network-based analysis of LiDAR penetration descriptors, the approach effectively estimates canopy parameters. The method was validated through simulation using diverse 3D canopy models, achieving performance metrics: RMSE: 0.2 m^2/m^3, R^2: 0.95 for LAD and RMSE: 0.17 m^2/m^2, R^2: 0.84 for LAI. Results confirm the potential of LiDAR-based systems for precise orchard canopy monitoring.

Keywords: Tree phenotyping, leaf area index, deep learning, proximal sensing robots, gap fraction

Introduction

The LAI, which quantifies leaf area per unit ground surface, is a critical metric in agriculture, underpinning processes such as photosynthesis, transpiration, and carbon fixation (Asner et al., 2003). In agricultural systems like orchards, LAI guides targeted interventions like pruning, irrigation, and pesticide application (Anthony et al., 2020; Stagno et al., 2024), enhancing yield and resource efficiency (Sun et al., 2024). Among the indirect methods, LiDAR stands out for its high spatial resolution and resistance to light and weather conditions, generating superior 3D point clouds for LAI estimation, outperforming traditional techniques such as LAI-2200 and digital hemispheric photography. (Wei et al. 2020) highlight its effectiveness in handling canopy complexity, providing reliable estimates even in heterogeneous systems, while addressing challenges like foliage clumping and occlusions. Beyond LAI, leaf area (LA), representing the total leaf surface, and LAD, defined as the leaf area per unit canopy volume, provide valuable insights into canopy structure. Although metrics like tree area index (TAI), which represents the total projected area of trees per unit ground area, and effective LAI (eLAI), a corrected estimate of leaf area accounting for foliage clumping and non-photosynthetic surfaces, offer additional perspectives, this study focuses on LAD, LA, and LAI due to their direct relevance to orchard management and their emphasis on foliage rather than structural elements like branches or trunks.

Current methodologies for LiDAR-based LAI estimation employ a variety of approaches, each with distinct strengths and limitations (Wang and Fang, 2020). Gap-based models, rooted in the Beer-Lambert law, estimate LAI by correlating gap fractions with LAD, whereas contact-based methods rely on the frequency of laser beam interception, using voxelised models to partition the canopy into horizontal layers (Weiss et al, 2004). Despite their simplicity and grounding in well-established physical

principles, gap-based and contact frequency models often struggle with inaccuracies caused by saturation effects, assumptions of canopy homogeneity and dependence on specific calibration of leaf projection function "G" (Yan et al,. 2019), which plays a critical role in these models, as it represents the average projection of leaf area in a given direction, relative to the total leaf area. Biophysical regression models establish empirical relationships between LiDAR-derived metrics—such as canopy height and density—and field-measured LAI. However, although allometric equations offer flexibility, adapting to specific vegetation types, yet their applicability is limited to the contexts for which they are calibrated. Machine learning methods, in turn, excel in capturing complex, non-linear relationships, providing both high accuracy and scalability (Zhang et al, 2019; Neuville et al, 2021). Nevertheless, their effectiveness hinges on the availability of extensive, high-quality datasets and significant computational resources. Bridging these approaches, integrating machine learning algorithms with modern data acquisition platforms presents a key area of focus. This synergy has the potential to significantly enhance the accuracy, scalability, and applicability of LAI estimation methods, particularly in diverse and complex ecosystems (Fang et al, 2019). The rapid development of agricultural robotics and the increasing use of unmanned ground vehicles (UGVs) are transforming the process of gathering detailed information about crops. UGVs equipped with LiDAR sensors represent a specific type of mobile laser scanner (MLS), also commonly referred to as mobile terrestrial laser scanner (MTLS), offering significant advantages, including the ability to autonomously navigate complex terrains and perform high-resolution, repeatable scans of crop canopies and structures. Unlike fixed platforms, UGVs are not constrained by spatial limitations, enabling large-scale, efficient data collection. This capability not only facilitates precise characterisation of canopy structures but also addresses key challenges such as data consistency, objectivity, and accessibility within crop canopies, which are often inaccessible to remote sensing methods (Rui et al., 2024).

Despite the advancements, current methods often overlook valuable information related to data acquisition processes, such as multi-perspective scanning of the canopy or the natural radiometric properties captured by sensors. This highlights the need for methods that effectively leverage LiDAR data while maintaining adaptability to diverse environmental and operational conditions. To address these challenges, this study presents a novel framework for LAD estimation, based on the integration of an UGV-based MLS, 3D LiDAR data, and neural networks. The proposed integration offers several advantages: (1) enabling multi-perspective scanning of canopy regions, capturing data from various distances and angles of incidence, (2) incorporating radiometric data and penetration descriptors, complementing the absolute coordinate space; and (3) using neural networks trained on balanced datasets to interpret non-linear relationships, adapting to variations in canopy structure and foliage density. This study aims to improve the LAD estimation by focusing on the following specific objectives:

i. To develop a pipeline for LAD estimation that integrates both absolute and local frame information derived from LiDAR data.
ii. To identify and evaluate key features for LAD estimation by evaluating the predictive performance of different feature groups extracted from the LiDAR data.
iii. To validate the proposed framework through simulations, assessing its accuracy and robustness across varying canopy structures and densities.

Materials and methods

This study employs a structured workflow to estimate LAD variations within the canopy and the overall tree LAI using simulated data. The overall workflow, as illustrated in Figure 1, comprises three key stages: data generation, extraction of local features, 3D reconstruction in absolute frame and model training and validation.

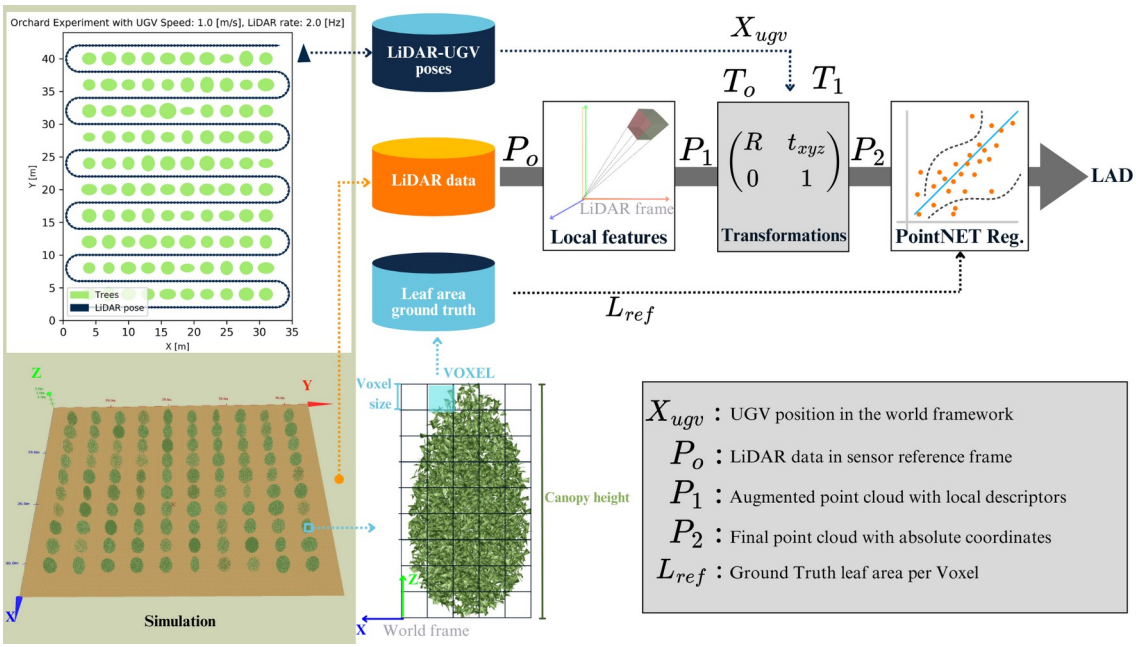

Figure 1. Methodological workflow for data generation and model development for LAD estimation

Data generation — A synthetic dataset was generated using simulated 3D tree canopy models and LiDAR responses. The discrete anisotropic radiative transfer (DART) model was employed to simulate LiDAR scans of 100 tree canopies with ellipsoidal shapes (Gastellu-Etchegorry et al., 2004). The LiDAR parameters in the DART software were configured as follows: a forward light propagation model, multiple pulse mode with discrete return, and output intensity values using Gaussian decomposition integral. The simulation was conducted using 24 species, comprising 12 distinct leaf angle distribution models: DeWit, bounded uniform, uniform, spherical, erectophile, planophile, extremophile, plagiophile, horizontal, vertical, ellipsoidal with average leaf angle of 55°, and elliptical (θ_m=50°, ε=0.6). Each model was simulated with two parameter sets $[a, b, \Omega_{min}, \Omega_{max}]$, resulting in 24 unique species variants. The first parameter set used values of $[1,1,0,0]$, while the second set used $[0.3,0.8,0.5,30]$, resulting in 24 unique species variants. The projection function is defined as follows, representing leaf angle distribution relative to incoming radiation:

$$G = \frac{\Omega_{max}}{1+\exp\left[-a.\left(\theta_n - b\right)\right]} + \Omega_{min} \qquad (1)$$

where, Ω_{max} and Ω_{min} are maximum and minimum values of the function; a is the controls the slope of the function, i.e., how quickly it changes with respect to θ_n, which is the zenith angle of incoming radiation or observation.b is the angle around which the main transition occurs.

Figure 2 presents histograms for the 100 generated tree canopies. The first plot shows the distributions of canopy width, canopy length [m], and canopy height [m] as overlapping histograms, while the second displays the total leaf area [m²]. The third plot highlights the distribution of species IDs, with selected labels omitted for clarity. These visualizations illustrate the variability and balance across key canopy traits and species identifiers.

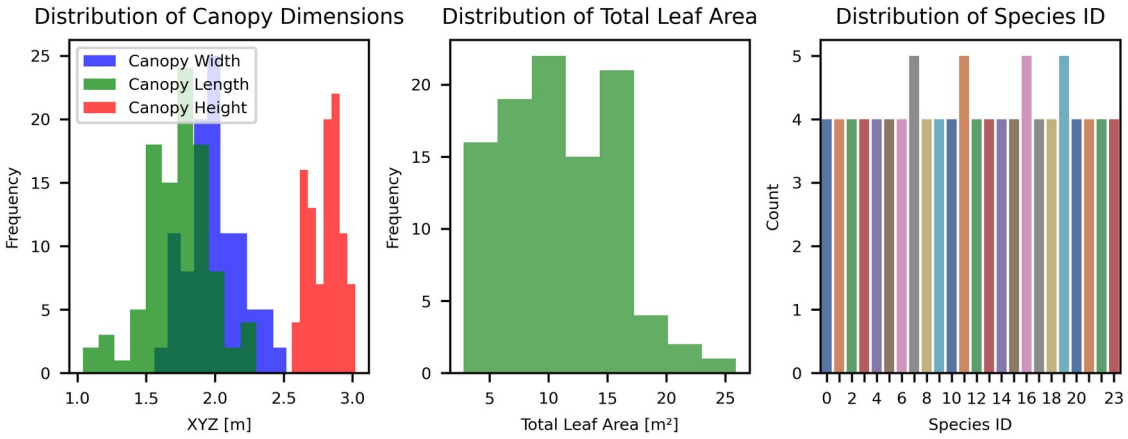

frame F_s, the UGV frame F_{ugv}, and the world frame F_w. Knowing the transformation T_o from the sensor frame to the UGV frame, and the UGV's position X_{ugv} in the world frame, the transformations T_1 (UGV to world) and T_1^{-1} (world to UGV) enable seamless coordinate transformations between all frames. This allows precise alignment and efficient data manipulation across the sensor, UGV, and world coordinate systems.

Local features – Each LiDAR scan S_t, where t represents time, consists of two components: $P_o \in \mathbb{R}^{n\times 3}$, representing the spatial coordinates (x, y, z) and $P_e \in \mathbb{R}^{n\times 3}$ with additional attributes: I_{raw} (raw intensity), $I_\rho = I_{raw}/\rho^2$ (distance corrected intensity) and N_e (number of echoes per beam). A novel approach to descriptor analysis was applied in the sensor frame F_s, focusing on integrating the beam's origin into the point cloud data. The local analysis aims to extract features that capture the origin and incidence angles of each beam in its natural frame. This contrasts with conventional point clouds, which only encode absolute (x, y, z) coordinates, neglecting local geometric and angular context. Each LiDAR scan was processed to extract local features, starting with the conversion of Cartesian coordinates into spherical coordinates (ρ, θ, ϕ), enabling precise analysis of angular deviations and geometric relationships. For each point within the scan, a curved voxel with a radius of 0.3 m was defined around the central point. Within this defined space, key local descriptors, including the local gap fraction (G_f), were calculated. (G_f) was determined as the ratio of beams passing completely through the voxel (N_p) to the total number of beams (N_t) interacting with the voxel, either by passing through or colliding inside its volume (N_i). Additionally, incidence properties, such as the number of echoes per beam (N_e) were determined. These attributes captured detailed structural characteristics of the canopy by quantifying light penetration and beam interactions. Once all scans had been processed, the data were accumulated into a final matrix that combined absolute coordinates with derived local descriptors, thereby expanding the information channels for each point from the point cloud. This dataset was subsequently partitioned into subsets for training

(60%), validation (20%), and testing (20%), ensuring an adequate balance for model training and evaluation. Figure 3 shows an example of the calculation of light beam counts passing through and contained within a curved voxel for a single 3D LiDAR scan point. In blue, the origin of F_s; in green, beams within the curved voxel; and in red, beams passing through it. Target LAD values were derived by voxelising the DART-generated reference data into 0.05-meter cells, calculating LAD based on the occupied volume, and scaling them according to voxel volumes. This comprehensive dataset served as the basis for training and evaluating the neural network model.

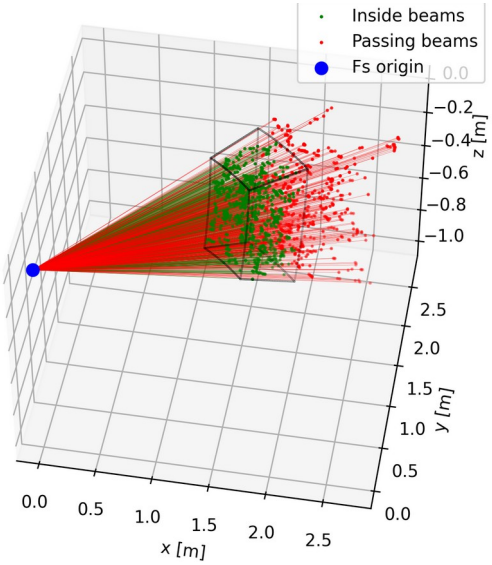

Figure 3. Determination of local gap fraction information within the curved voxel for beam -i, defined as a section of space in spherical coordinates with sensor frame origin.

Neural network regression framework – This study employs a regression model inspired by PointNet (Qi et al., 2017), designed for processing 3D point clouds. The model utilizes spatial transformer networks (STN) for input alignment and feature transformation, followed by convolutional layers for feature extraction and fully connected layers for regression. The input comprises Cartesian spatial coordinates (x, y, z) and allows the incorporation of additional features such as radiometric descriptors derived from LiDAR (I_{raw}, I_p, N_e), local sensor frame data in spherical coordinates (ρ, θ, ϕ) and attributes determined from curved voxels (N_p, N_i, N_t, G_f).

LAI determination – Tree LAI is computed by integrating the predicted LAD across all the involved voxels N_{vox}. The LAI is consequently related to the projected area of each individual tree, without considering the planting frame, i.e., the number of plants per unit area:

$$LAI = \frac{1}{A_p} \sum_{i=1}^{N_{vox}} LAD_i \cdot Voxel_{vol} \quad (2)$$

where, LAD_i is prediction for voxel -i and $Voxel_{vol}$ is the curved voxel volume. This implies the necessity of a 3D tree segmentation process to isolate individual trees. A_p is the ground-projected tree area, derived from voxel x-y information, and does not account for the number of trees per unit ground area.

Results

The framework was tested to estimate LAD and LAI, with R^2 and RMSE quantifying accuracy and feature contributions supporting its validity. Figure 4 presents the test results for feature addition analysis, evaluating the impact of progressively combining the base spatial features with individual descriptors: radiometric-aided, local spatial-aided, local gap fraction-aided, and the full feature set.

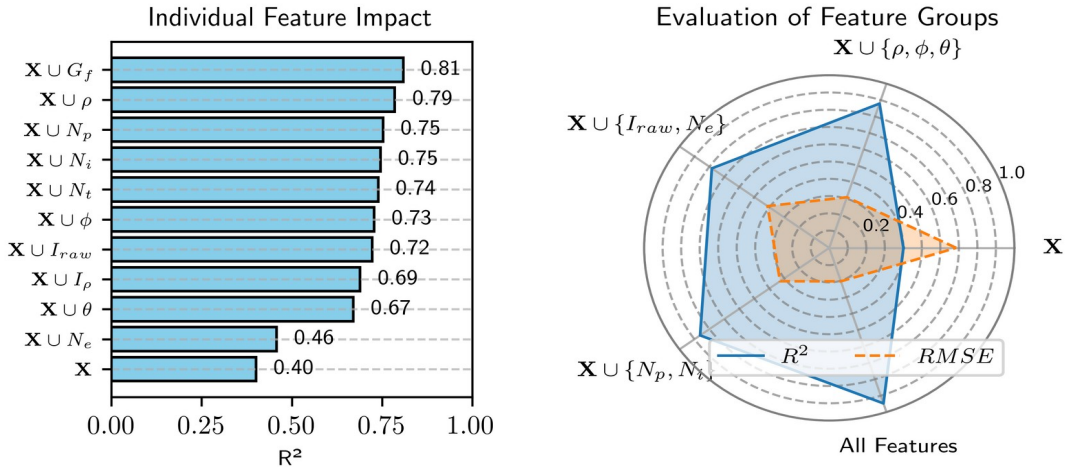

(a) (b)

Figure 4. Performance evaluation of LAD estimation based on features: (a) evaluation of individual feature impact, and (b) evaluation of groups. Where $X = \{X, Y, Z\}$

Using the selected feature space $X \cup \{I_{raw}, \rho, \theta, N_t, G_f\}$, Figure 5a presents the model's performance in LAD estimation, showcasing a strong correlation between predicted and reference values. Subsequently, the framework was applied to estimate LAI across 100 trees on a second experiment, with the results summarized in Figure 5b.

Discussion

The proposed framework demonstrated potential for enhancing LAD and LAI estimation in orchard systems by integrating LiDAR data, UGVs, and neural network-based regression models. The results, validated through simulations, achieved high accuracy metrics (R^2=0.95 and RMSE = 0.2 m²/m³ for LAD; R^2=0.84 and RMSE = 0.17 m²/m² for LAI), indicating the framework's ability to capture canopy structural properties effectively.

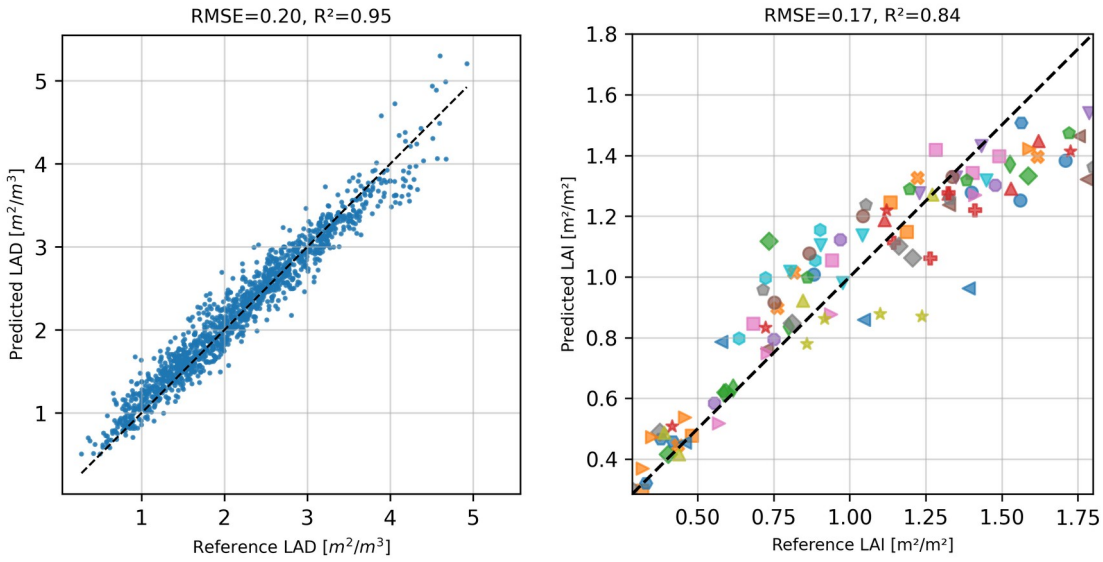

(a) (b)

Figure 5. Testing performance: (a) LAD estimation with full features space and (b) Tree LAI estimation with 24 foliage distributions shown by shapes and colour.

These findings align with previous studies while addressing limitations, such as the lack of multi-perspective data acquisition. Unlike traditional machine learning methods in the literature, which rely on tree-level metrics such as height, crown diameter, or volume to estimate leaf area properties, the proposed regression approach analyses data at the voxel scale. The method can generate estimations of tree-level metrics, providing both, a detailed spatial representation on LAD and total LAI. However, it is important to note that the accumulation of error in the LAD estimation also contributes to an error in the overall LAI metric. Furthermore, in regions with higher foliage density, the reduction in available data due to occlusions and the increased likelihood of saturation from limited laser penetration may also contribute to estimation errors.

Conclusions

This study explored the potential of integrating LiDAR data, UGV platforms, and neural networks for estimating LAD and subsequently LAI in orchards. The proposed framework, validated on simulated data, achieved high accuracy, showcasing its capacity to capture canopy structural information. By making LAD predictions at the voxel level derived from multiple platform perspective, the method enhances the precision of canopy characterization. The findings demonstrates that incorporating supplementary information at point scale, such as penetration descriptors (e.g., gap fraction at the local frame of reference), distance to the voxel, angle of incidence, or radiometric sensor data, can significantly enhance the performance of the prediction model.

Future efforts should focus on testing the framework using real-world datasets to evaluate its practical utility in orchard systems.

Acknowledgements

This research was supported by LAAS-CNRS, Toulouse, France, in collaboration with the Universidad de Ibagué, Colombia. The authors gratefully acknowledge financial support from “Fundación para el Futuro de Colombia” Colfuturo.

References

Anthony, B., Serra, S. and Musacchi, S., 2020. Optimization of light interception, leaf area and yield in "WA38": comparisons among training systems, rootstocks and pruning techniques. Agronomy, 10(5), 689.

Asner, G.P., Scurlock, J.M. and A. Hicke, J., 2003. Global synthesis of leaf area index observations: implications for ecological and remote sensing studies. Global ecology and biogeography, 12(3), 191-205.

Fang, H., Baret, F., Plummer, S. and Schaepman-Strub, G., 2019. An overview of global leaf area index (LAI): Methods, products, validation, and applications. Reviews of Geophysics, 57(3), 739-799.

Gastellu-Etchegorry, J.P., Martin, E. and Gascon, F., 2004. DART: a 3D model for simulating satellite images and studying surface radiation budget. International Journal of Remote Sensing, 25(1), 73-96.

Neuville, R., Bates, J.S. and Jonard, F., 2021. Estimating forest structure from UAV-mounted LiDAR point cloud using machine learning. Remote sensing, 13(3), 352.

Qi, C.R., Su, H., Mo, K. and Guibas, L.J., 2017. Pointnet: Deep learning on point sets for 3d classification and segmentation. In Proceedings of the IEEE conference on computer vision and pattern recognition, 652-660.

Rui, Z., Zhang, Z., Zhang, M., Azizi, A., Igathinathane, C., Cen, H., et al., 2024. High-throughput proximal ground crop phenotyping systems–A comprehensive review. Computers and Electronics in Agriculture, 224, 109108.

Stagno, F., Brambilla, M., Roccuzzo, G. and Assirelli, A., 2024. Water Use Efficiency in a Deficit-Irrigated Orange Orchard. Horticulturae, 10(5), 498.

Sun, G., Chen, S., Zhang, S., Chen, S., Liu, J., He, Q., et al., 2024. Responses of leaf nitrogen status and leaf area index to water and nitrogen application and their relationship with apple orchard productivity. Agricultural Water Management, 296, 108810.

Wang, Y. and Fang, H., 2020. Estimation of LAI with the LiDAR technology: A review. Remote Sensing, 12(20), 3457.

Wei, S., Yin, T., Dissegna, M.A., Whittle, A.J., Ow, G.L.F., Yusof, M.L.M., et al., 2020. An assessment study of three indirect methods for estimating leaf area density and leaf area index of individual trees. Agricultural and Forest Meteorology, 292, 108101.

Weiss, M., Baret, F., Smith, G.J., Jonckheere, I. and Coppin, P., 2004. Review of methods for in situ leaf area index (LAI) determination: Part II. Estimation of LAI, errors and sampling. Agricultural and forest meteorology, 121(1-2), 37-53.

Yan, G., Hu, R., Luo, J., Weiss, M., Jiang, H., Mu, X., et al., 2019. Review of indirect optical measurements of leaf area index: Recent advances, challenges, and perspectives. Agricultural and Forest Meteorology, 265, 390-411.

Zhang, L., Shao, Z., Liu, J. and Cheng, Q., 2019. Deep learning based retrieval of forest aboveground biomass from combined LiDAR and landsat 8 data. Remote Sensing, 11(12), 1459.